

Experimental analysis of an innovative prosthetic hand with proprioceptive sensors

M.C. Carrozza*, F. Vecchi†, F. Sebastiani†, G. Cappiello†, S. Roccella†, M. Zecca*, R. Lazzarini* and P. Dario*

*ARTS Lab - Scuola Superiore Sant'Anna, Polo Sant'Anna Valdera
viale Rinaldo Piaggio, 34 - 56025 Pontedera (PI), Italy

†Centro INAIL RTR, via Vetraia, 7 - 55049 Viareggio (LU), Italy

Email: chiara@mail-arts.sssup.it

Abstract—This paper presents an underactuated artificial hand intended for functional replacement of the natural hand in upper limb amputees. The natural hand has three basic functionalities: grasping, manipulation and exploration. To accomplish the goal of restoring these capabilities by implanting an artificial hand, two fundamental steps are necessary: to develop an artificial hand equipped with artificial proprioceptive and exteroceptive sensors and to fabricate an appropriate interface able to exchange sensory-motor signals with the amputee's body and the central nervous system. In order to address these objectives, we have studied an underactuated hand according to a biomimetic approach, and we have exploited robotic and microengineering technologies to design and fabricate its building blocks. The architecture of the hand comprises the following modules: an actuator system embedded in the underactuated mechanical structure (artificial musculoskeletal system), a proprioceptive sensory system (position and force sensors), an exteroceptive sensory system (3D force sensors distributed on the cosmetic glove), an embedded control unit (low level control loop dedicated to control incipient slippage and grasping), and a human/machine interface (a EMG control unit to enable the amputee to control the artificial hand). The first prototype of the artificial hand has been designed and fabricated. The hand is underactuated (9 degrees of freedom controlled by two actuators), and is equipped with opposable thumb and a proprioceptive sensory system. This paper presents the fabrication and experimental characterization of the hand, focusing on the mechanical structure, the actuator system and the proprioceptive sensory system. The grasping and sensing capabilities of the first prototype have been experimentally tested with an innovative method to estimate the grasping force, and preliminary results are presented and analyzed.

I. INTRODUCTION

This paper describes an underactuated artificial hand for functional replacement of the natural hand. The hand is composed of: an actuator system embedded in an underactuated mechanical structure (artificial musculoskeletal system), a proprioceptive sensory system (position and force sensors), an embedded control unit (low level control loop dedicated to control the incipient slippage and the grasping), and a human/machine interface (a EMG control unit to enable the amputee to control the artificial hand). The paper also illustrates the results of experimental tests aimed at evaluating the

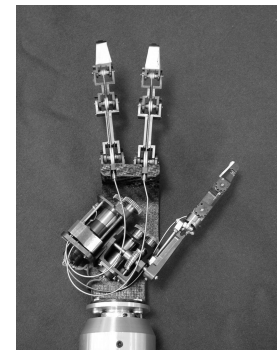
force and grasping performance of the hand prototype.

II. MECHANICAL STRUCTURE

The design goal of the mechanical structure is to enable a stable grasp with objects of different size, texture and shape, without augmenting the mechanical and the control complexity. For this reason, the hand (called "RTR II") has an opposable thumb able to adduct and abduct, and to adapt to different grasps. The design approach of the RTR II hand exploits underactuated mechanisms as described in detail in a previous paper [1]; in particular the solution proposed by Shigeo Hirose in the Soft Gripper [2] has been applied to both fingers and thumb.



(a)



(b)

Fig. 1. The RTR II prosthetic hand (a) and the actuation and transmission system of the RTR II hand (b).

Underactuated mechanisms allow to obtain self-adaptive grasping capabilities, thanks to a large number of degrees of freedom (DOFs) controlled with a limited number of actuators and differential mechanisms. This feature is particularly important in prosthetic hands, when only few control signals are available from the EMG Control Interface, and therefore it is not possible for the amputee to control more than two actuators. The hand has three fingers, the middle, the index and the thumb, but only two motors: one for the flexion and extension movements of all the fingers and the thumb (power

grasp) and one for the adduction and abduction movements of the thumb (precision grasp). Index and middle fingers are identical (both have three phalanges), while the thumb has two phalanges, as the human hand (see Fig. 1 (a)). The hand is based on a tendon transmission system. The tension of the tendons generates a flexing torque around each joint, by means of small pulleys, and allows the flexion movement; the extension movement is realized by torsion springs. The adduction and abduction movements of the thumb are realized by means of a four bar link mechanism. Fig. 1 (b) shows the actuation and the transmission systems.

III. SENSORS

The artificial sensory system is the core of the hand control system, and has a twofold function: first, it provides input signals for the low-level control loop of the grasping phase, thus enabling local and autonomous control of the grasp without requiring user's attention and reaction to incipient slippage. Moreover, the ultimate function of the artificial sensory system is to generate sensory signals to be transmitted to the user through an appropriate neural interface (high-level control loop) when it will be available in the future. For the moment, the user will be able to control the hand in a direct, fast and instinctive way through EMG signals generated at the residual forearm. The low-level control system increases the grasping force as soon as incipient slippage occurs and the object is going to slip, and thus it replicates natural user's reaction without requiring his/her attention and specific effort. The ideal control requires a simple starting command to perform a secure grasp, independently of the specific object characteristics in terms of shape, size and texture. The human hand is able not only to perform grasping tasks but also to estimate the weight, the texture and the temperature of the grasped object. The natural sensory feedback could be restored, to some degree, mainly in two different ways:

- by exploiting other senses (e.g. the sense of sight, the sense of hearing or the sense of touch in other parts of the body) as input channels for the information provided by the prosthesis sensors;
- by establishing some communication channels with the Central Nervous System (CNS) by electrically connecting in vivo to nerve endings.

Provided that neural interfaces become available, and implants are feasible and reliable, it is obvious that the second choice can be the optimal solution. These issues are addressed in specific projects aimed at developing a Cybernetic Hand [3]. It is clear that prosthetic hands should be equipped with artificial-sensory systems specifically intended to transmit sensing signals to the neural interface. Different types of sensing technologies have been developed and some of them can be exploited for fabricating artificial proprioceptors. For example it is possible to obtain position sensors based on encoders or potentiometers [4]–[6], Hall effect sensors [7] [8], and force feedback sensors usually based on strain gages [5], [6], [8]–[10]. In order to solve the problem of force

and position measurements in the RTR II hand, the cable transmission is sensorized with strain gage and Hall effect sensors as described in detail in the following sub-section.

A. Force and Position Sensors

In the RTR II hand, the transmission cables are fixed on one end to the index and middle distal phalanges and, on the other end, they are connected to the linear slider through the two compression springs of the differential mechanism. The cables act directly on two mobile elements, which compress the springs during the adaptive grasp of an object of irregular shape. The force sensor is obtained by sensorizing an elastic element acting as a mechanical stop for the cables. The mechanical structure of the mobile elements has been designed to obtain a deformable cantilever, as shown in Fig. 2, where two semiconductor strain gages (Entran[®], Entran Devices, Inc., Fairfield, NJ, USA) detect strains.

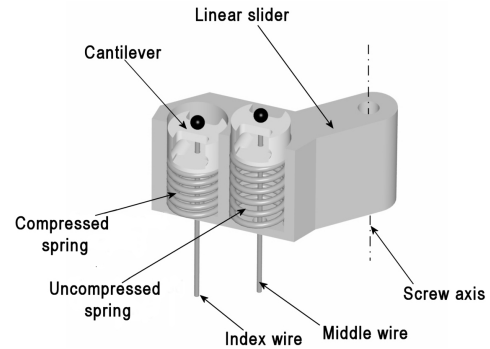


Fig. 2. Cross section of the linear slider. The value of cable tension is estimated through the measurement of the elastic deformation of the cantilevers realized on the mobile elements.

Table I summarizes the main specifications of the semiconductor strain gage used. It can be observed that it has small dimensions, very useful characteristic for this application.

TABLE I
CHARACTERISTICS OF THE ESU-025-1000 STRAIN GAGE BY ENTRAN[®],
ENTRAN DEVICES, INC., FAIRFIELD, NJ, USA).

Model Name	ESU-025-1000
Shape	U
Nominal Resistance (20°C)	1000Ω
Nominal Thermal Coefficient of Resistance (55°C)	+22%
Nominal Gage Factor (20°C)	155 ± 5%
Nominal Thermal Coefficient of Gage Factor (55°C)	-18%
Gage Type	P-Type Silicon
Strain Level	0 – 1000μstrain recommended, 0 – 3000μstrain maximum
Dimensions	1.27x0.38 mm

The mobile elements have been designed according to the results of a finite element modelling obtained with the software Ansys[®] Multiphysics (ANSYS Inc. Corporate, Canonsburg, PA, USA), considering a maximum load of 40 N applied by the cable. The strain values parallel to the cantilever

axis are always lower than $1000\mu\text{strain}$, with an average of $200\mu\text{strain}$: this means that the mobile elements have been designed in such a way that their deformation is always in the elastic range. Stress values are far from the limit imposed by the steel tensile strength. Simulation has allowed to find the optimum position of the strain gage sensors on the mechanical stop. An experimental calibration of the force sensor has been made with an external sensor, in order to correlate the cable tension with the internal sensor output. The calibration has been performed with an INSTRON[®] 4464 test machine (Instron Corporation, Canton, Massachusetts, USA) with a static load cell working in the range of ± 1 KN. A cone-shaped tip, fixed to the load cell, has been used to apply the load, as shown in Fig. 3 (top). The strain gage sensors signal has been first amplified, then acquired through an acquisition board (National InstrumentsTM DAQ Card 1200), and finally processed by a custom LabVIEWTM interface to visualize in real time its output (Volts) versus the applied load (N).

Fig. 3 (bottom) shows some linearity error caused mainly by the error introduced during the assembly of the mobile element on the support, and the assembly of the cone-shaped tip on the load cell.

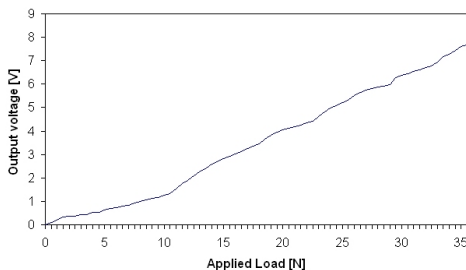
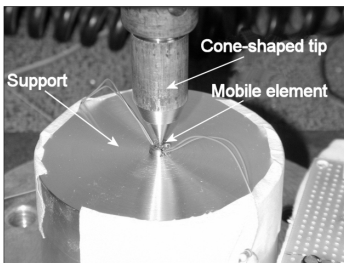


Fig. 3. A cone-shaped tip applied the load deforming the cantilever realized on the mobile element (top). Data obtained during sensor characterization. Output voltage of the internal sensor versus applied load measured with an external sensor (bottom).

This error can be limited by reducing the machining and assembling tolerances. However the curve is monotonic so the output voltage can be calibrated with the applied load via software, making possible to uniquely and directly estimate the applied load by measuring the internal sensor output.

The position sensor suitable for this application should have small size, low power consumption and should be absolute, to avoid a zero setting procedure each time the prosthesis is turned on. Hall effect sensors meet these requirements and

have been exploited for detecting cable slider position. They have been glued (the sensor used is the *SS496B* by Honeywell International Inc.) to the linear slider and small magnets have been attached to the palm to create the magnetic field.

IV. HUMAN-MACHINE INTERFACE: PROCESSING OF THE EMG SIGNAL

The user can control the grasping task by means of two EMG signals generated by two antagonist muscles of the forearm devoted to the wrist flexion-extension movement: the *extensor carpi radialis* and the *flexor carpi radialis*. The signals are acquired and processed by two small boards (each 0.8" by 1.5" in dimension), shown in Fig. 4: in the first board, the signal is rectified and filtered (pre-processing phase); in the second one, the pre-processed EMG-signal is used to control the actuators of the RTR II hand (low level control). The function of the two boards is to interpret the user's intention and to send the appropriate commands to the actuators.

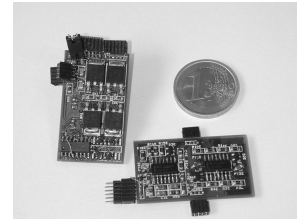


Fig. 4. Two small boards are used to preprocess the EMG signal and to control the actuators of the RTR II hand.

A. EMG pre-processing

The first board receives as inputs two EMG signal measured by 2 Delsys DE2.3 differential Ag electrodes (Delsys Inc., Boston, MA, USA), designed with a built-in gain of 1000 V/V and a built-in pass band filter from 20 ± 5 Hz to 450 ± 50 Hz. These signals are then rectified (by a full-bridge precision rectifier with adjustable gain) and low-pass filtered through a Butterworth filter (2^{nd} order, pass-band edge frequency: 8 Hz, pass-band attenuation: 0.5 dB, $f_p=13.56$ Hz), whose transfer function is:

$$T(s) = T_0 \frac{A}{Bs^2 + Cs + D} \quad (1)$$

where $T_0 = 1$, $A = 7.23E3$, $B = 1$, $C = 1.2E2$, $D = 7.2E3$.

The two rectified signals are then compared in order to detect the direction of movement (i.e. extension=open, flexion=close; *SGN* signal); moreover, the signal is also compared with an adjustable threshold with a regenerative comparator, in order to detect if there is a movement or not (*EDG* signal).

B. Low level control of the hand

The second board receives 3 signals from the first one: activation (*EDG*), direction (*SGN*) and amplitude of the movement (*AMP*). The first signal (*EDG*) is used to understand if there is a movement or not; the 2^{nd} (*SGN*) to

choose between opening and closing, and the 3rd (*AMP*) to control the speed of the movement in a proportional way. The second board is composed of 2 blocks: the control block, which is composed by a PIC16F870 microcontroller, and the driver block, which contains 2 drivers capable of driving 2 motors up to 18W each.

The control algorithm (in this first prototype) is a simple proportional open loop control. It remains in the stand-by state (low power consumption) until there is a positive edge of the *EDG* signal. The controller reads the *SGN* signal (*SGN*₀), and starts to sample the *AMP* signal (obtained by the rectified difference of the 2 rectified EMG signals). After *t*_{wait} (*t*_{wait}=300msec in this first version of the controlling algorithm) the controller reads once again the *SGN* signal (*SGN*₁). If *SGN*₁ ≠ *SGN*₀, it means that the user is changing the control from one motor to the other. Instead, if *SGN*₁ = *SGN*₀, the controller starts to drive the motor of the hand by using the Pulse Width Modulation (PWM) technique. The duty cycle is calculated from the average of the previous 64 samples of the EMG signal. The direction of movement is determined by the *SGN* signal. During *t*_{wait} the microcontroller samples the EMG signal, and averages the last 128 samples. If this average is greater than a pre-determined threshold for more than 70% of the time, it means that the user wants to move the hand at low speed. The next version of the control algorithm, currently under development, will exploit the force and position sensors, in order to control locally some grasping functions.

V. EXPERIMENTS

A. Analysis of the force and position sensors

1) *Force sensor*: A cylindrical object, suitably designed and developed to contain the uniaxial load cell Futek[®] L1650 (FUTEK Advanced Sensor Technology, Inc., Irvine, CA, USA) has been used as a dynamometer to calibrate the force sensor with the hand grasping force, as shown in Fig. 5.

During the grasping phase of the cylindrical object, the output of the load cell has been collected and compared with the output of the force sensor (see Fig. 6).

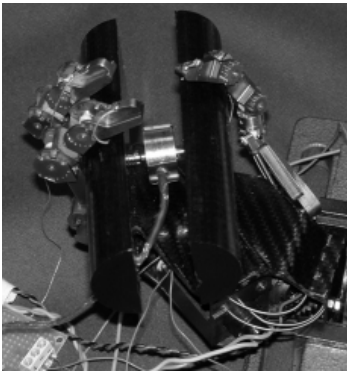


Fig. 5. To measure the grasping force of the RTR II hand, a cylindrical object, containing an uniaxial load cell, has been developed. The force sensor has been calibrated comparing its output with the load cell one.

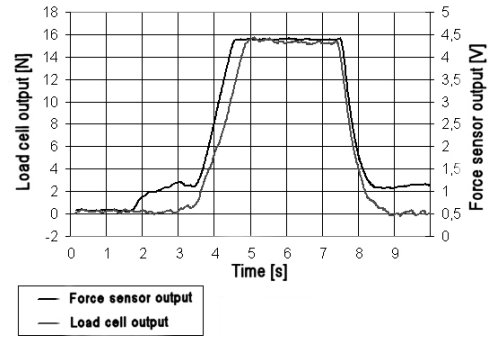


Fig. 6. The load cell output and the force sensor output versus time, with a motor supply of 1A. It is possible to see the grasping phase, the grasp maintenance once the motor supply is turned off, and the releasing phase.

In the first part of the curve, shown in Fig. 6, only the cable tension increases while the force acting on the object, i.e. the load cell output, is close to zero. In this phase the cable tension compresses the springs inside the differential mechanism to obtain a complete adaptation of the fingers to the object shape. The second part of the curve is quite linear and it shows how the grasping force and the cable tension increase in the same way. After a constant part, when the hand is holding the grasp once the motor supply is turned off, there is a decreasing part of the curve, corresponding to the releasing phase, and there is another delay between the force sensor output and the load cell output, which again is due to the action of the compression springs.

The force sensor output has been calibrated using four maximum current levels: 0.3A, 0.5A, 0.75A, 1A. Table II shows the different operative ranges of the force sensor output and the linearity errors of its calibration curves.

TABLE II
FORCE SENSOR CALIBRATION.

mA	Force Sensor Output [V]	Measured Grasping Force [N]	Linearity error (%FSO)
300	1 - 2.8	0.4 - 6.5	5.4%
500	2.7 - 4.4	0.6 - 10.2	1.8%
750	1 - 4.5	1 - 15.1	5.7%
1000	1.2 - 4.4	1 - 15.6	6.6%

After this calibration procedure, the force sensor output can be directly used to estimate the total grasping force of the RTR II hand during a cylindrical grasp.

2) *Position sensor*: The main problem encountered when developing a position sensor, was to cover the entire slider's stroke (about 20 mm) which is large compared to the normal working range of Hall effect sensors; for this reason we have simulated and compared a number of different magnets configurations by means of the software Ansys[®] Multiphysics (ANSYS Inc. Corporate, Canonsburg, PA, USA). A specific optimal configuration has been experimentally found using 12 Honeywell International Inc. 103MG5 magnets. The Hall electrical tension generated in this configuration is able to cover the entire slider's stroke and its trend is monotonic and

quite linear, as shown in Fig. 7. A Matlab[®] (The MathWorks, Inc., Natick, MA, USA) model, described in [1], has been developed to correlate the slider position with the joints angles: through this model is possible to estimate the joints position during an opening-closure motion.

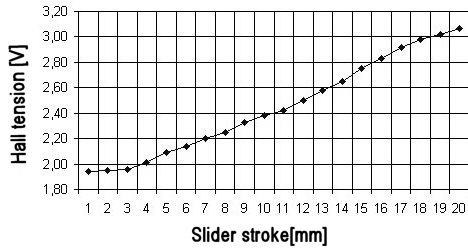


Fig. 7. Hall tension versus linear slider's stroke. Hall tension trend is monotonic and quite linear over the entire slider's stroke.

B. Grasp analysis

The ability of the RTR II hand to adapt to the shape of the grasped object allows to increase the number of contact points between the phalanges and the object and to augment the contact areas. In order to estimate the force applied when performing a power grasp of cylindrical objects, we have adopted an innovative experimental approach based on friction coefficient estimation, as described in detail in [11].

1) *Estimation of the generalized grasping force:* The objective of this experimental test is to estimate the *generalized grasping force* exerted by the RTR II hand when performing power grasps of cylindrically shaped objects at various levels of motor current supply.

a) *Experimental test description:* In order to monitor the force applied to the object ($F_{applied}$) and calculate its maximum value as soon as slippage occurs, we decided to fix the object directly to the static load of the INSTRON[®] 4464 test machine (Instron Corporation, Canton, Massachusetts, USA). Three cylinders (Delrin[®]) of different diameters (52mm, 67mm and 80mm), have been grasped by the RTR II hand in a supinated position, with the fingers axes perpendicular to the cylinder main axis (see Fig. 8). The contact areas have been covered with steel leafs (0,5mm of thickness). The resulting (static) coefficient of friction has been estimated in a previous work [11] and it is $\mu = 0.15 \pm 8.2\%$. It is important to note that the estimated friction coefficient does not depend on dragging velocity.

The load cell output has been calibrated and balanced, and the load application started by dragging the object at a constant velocity of 2mm/s. Five maximum current levels have been chosen: 0.25A, 0.5A, 1A, 1.5A and 2A, with a constant voltage level of 6V.

b) *Results:* Fig. 9 shows the typical time response of the load force measured by the load cell attached to the grasped cylinder. From experimental data it is possible to identify the instant when the slippage begins, and the corresponding maximum $F_{applied}$ which is used for the estimation of the generalized grasping force [11].

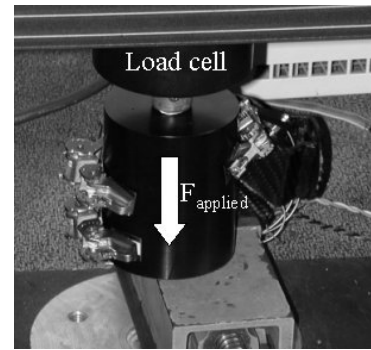


Fig. 8. The experimental set up for the estimation of the generalized grasping force.

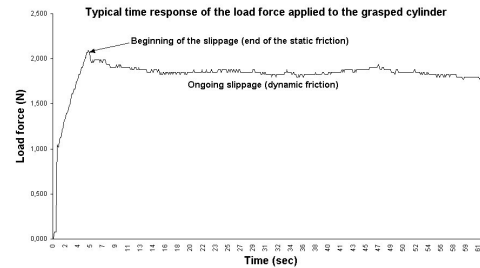


Fig. 9. Load force versus time when constant current was supplied to the motor and the grasped object is pull down with a constant velocity. The force increases quite linearly until the beginning of the slippage, then, after a sudden decrease, it becomes quite constant.

The *generalized grasping force* generated by the RTR II hand during the grasping of cylindrical objects was calculated using the method described in [11]. Fig. 10 shows how the force increases versus motor supply. It is also evident that at low power supply the hand forces do not depend on cylinder diameters. A possible explanation of this behavior is that the excessive current supply causes a reduction of the number of contact points in case of cylinders with diameters smaller than 80mm, because of the increased flexion of the distal interphalangeal joint. The grasping force generated on a cylindrical object (diameter of 67mm) has been measured by means of the dynamometer presented in the section V-A.1. The results (see Fig. 10) have shown that the maximum error between the measured and the estimated values of the grasping forces is -14% of the Full Scale Output (15.2N at 1A).

C. Thumb force analysis

The objective of this experimental test is to measure the *grasping force* exerted by the thumb of the RTR II hand when performing the grasp in the lateral pinch configuration at various levels of motor current supply.

1) *Experimental test description:* The RTR II hand has been fixed in a supinated position and the thumb has been left free to realize the lateral pinch on the load cell of the INSTRON[®] 4464 test machine (Instron Corporation, Canton, Massachusetts, USA) that has been used as a dynamometer. Five maximum current levels have been chosen: 0.25A, 0.5A, 0.75A, 1A, and 1.5A, with a constant voltage level of 6V.

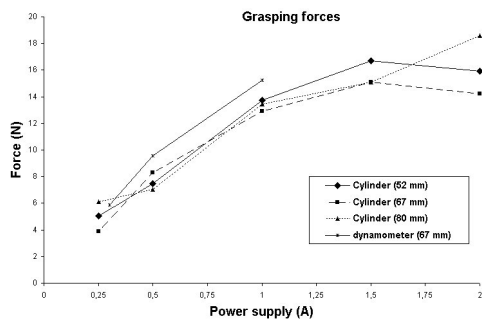


Fig. 10. Estimated grasping forces with different diameter objects and measured grasping force with a dynamometer vs Power supply (constant voltage= 6V).

After the first contact of the thumb fingertip with the load cell, some current spikes have been used in order to obtain the maximum level of force.

2) *Results:* Fig. 11 shows the force generated by the thumb during the lateral pinch versus motor supply. The force increases quite linearly up to 0.75A and reaches the maximum level (6.2N) with a current supply of 1A. It is also evident that thumb forces do not increase with higher levels of current supply.

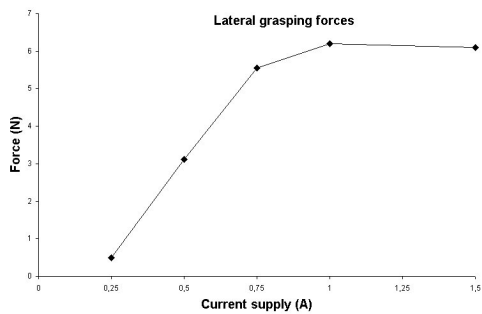


Fig. 11. Force generated by the thumb during the lateral pinch versus current supply.

The forces generated by the thumb during the lateral pinch depend on the number of current impulses supplied after the contact with the object. Fig. 12 shows how each current impulse leads a positive step for the force generated by the thumb. The smallest and the highest levels of current (0.25A and 1.5A) are two exceptions because of the corresponding force levels do not depend on current impulses. In order to obtain the highest force levels with the smallest power supply consumption, future studies will focus on designing and developing an optimal control strategy for the motors supply based on the use of current impulses.

VI. CONCLUSION

The objective of this paper is the description of an under-actuated hand for functional replacement of the natural hand. The proprioceptive sensory structure showed a good linearity and the next version of the control algorithm will exploit the force and position sensors to implement a closed-loop

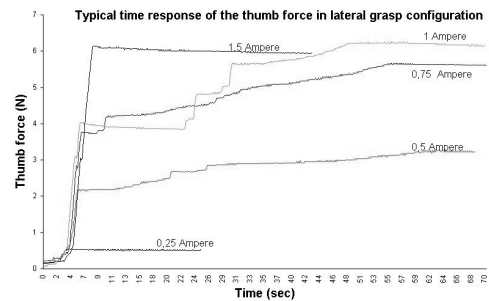


Fig. 12. In case of 0.5A, 0.75A, and 1A current supply, the maximum forces generated by the thumb fingertip depend on the number of current impulses supplied after the first contact with the object (constant voltage= 6V).

control of the hand. The maximum measured grasping force was 18N. Ongoing activity is focused on the fabrication of a second prototype of the RTR II hand in order to perform an experimental comparison with state of the art and commercial hand prostheses.

ACKNOWLEDGMENT

The authors would thank Bruno Massa for his valuable contribution to the design and development of the RTR II Hand. This work has been carried at the RTR Research Centre in Rehabilitation Bioengineering (Viareggio, LU, Italy) of the INAIL Prosthetic Centre funded by INAIL (National Institute for Insurance of Injured Workers), and originated by a joint initiative promoted by INAIL and by Scuola Superiore Sant'Anna.

REFERENCES

- [1] B. Massa, S. Roccella, M. C. Carrozza, and P. Dario, "Design and development of an underactuated prosthetic hand," in *Robotics and Automation, 2002. Proceedings. ICRA '02. IEEE International Conference on*, vol. 4, 2002, pp. 3374–3379.
- [2] S. Hirose and Y. Umetami, "The development of soft gripper for the versatile robot hand," *Mechanism and Machine Theory*, vol. 13, pp. 351–359, 1977.
- [3] The CYBERHAND Project (Development of a Cybernetic Hand, IST-FET Project #2001 – 35094).
- [4] Y. Matsuoka, "The mechanisms in a humanoid robot hand," *Autonomous Robots*, vol. 4, pp. 199–209, 1997.
- [5] J. Butterfas, M. Grebenstein, H. Liu, and G. Hirzinger, "DLR-hand II: Next generation of a dextrous robot hand," in *IEEE International Conference on Robotics and Automation*, 2001, pp. 109–114.
- [6] C. Lovchik and M. Diftler, "The Robonaut hand: A dexterous robot hand for space," in *Robotics and Automation, 1999. Proceedings. 1999 IEEE International Conference on*, vol. 2, 1999, pp. 907–912.
- [7] M. Carrozza, B. Massa, S. Micera, R. Lazzarini, M. Zecca, and P. Dario, "The development of a novel prosthetic hand – ongoing research and preliminary results," *IEEE/ASME Transactions on Mechatronics*, vol. 7, no. 2, pp. 108–114, Jun 2002.
- [8] A. Caffaz and G. Cannata, "The design and development of the DIST-Hand dextrous gripper," in *Robotics and Automation, 1998. Proceedings. ICRA '02. IEEE International Conference on*, 1998.
- [9] S. C. Jacobsen, J. E. Wood, D. F. Knutti, and K. B. Biggers, "The Utah/MIT hand: work in progress," *The International Journal of Robotics Research*, vol. 3, no. 4, pp. 21–50, 1984.
- [10] J. K. Salisbury and J. J. Craig, "Articulated hands: force control and kinematic issue," *The International Journal of Robotics Research*, vol. 1, no. 1, pp. 4–17, 1982.
- [11] M. C. Carrozza, C. Suppo, F. Sebastiani, B. Massa, F. Vecchi, R. Lazzarini, M. Cutkosky, and P. Dario, "The SPRING hand: development of a Self-adaptive Prosthesis for Restoring Natural Grasping," *Autonomous Robots*, (Submitted for publication).